Journal of Solid State Chemistry **155,** 22–28 (2000)
doi:10.1006/jssc.2000.8930, available online at http://www.idealibrary.com on IDEAL®

A Combined X-Ray and Neutron-Powder Diffraction Study of a Superstructure Derived from $Tl_{0.75}Sr_{1.8}Ba_{0.2}CuO_y$

M. O. Jones, I. Gameson, and P. P. Edwards[1]

School of Chemistry, The University of Birmingham, Edgbaston, Birmingham, B15 2TT, United Kingdom

and

C. Michel, M. Hervieu, and B. Raveau[1]

Laboratoire CRISMAT, ISMRA/Université de Caen, Boulevard du Maréchal Juin, 14050, Caen, France

Received March 23, 2000; in revised form August 3, 2000; accepted August 15, 2000

DEDICATED TO PROFESSOR J. M. HONIG

We have observed a superstructure derived from the compound $Tl_{0.75}Sr_{1.8}Ba_{0.2}CuO_y$. This compound arises from the "collapse" of the parent oxynitrate compound $TlSr_2Ba_2Cu_2O_7(NO_3)$ under controlled thermal decomposition. A combined X-ray and neutron powder diffraction study of the title compound indicates that the superstructure possesses the *Pmmm* space group, with unit cell parameters (derived from neutron diffraction data) of $a = 3.7362(3)$ Å, $b = 11.5449(9)$ Å, and $c = 9.1494(8)$ Å. This superstructure takes the form of a three-fold repeat along the crystal *b*-axis produced through local distortions of the thallium and barium/strontium positions. This compound is nonsuperconducting due to the presence of a large number of vacancies in the electronically active copper–oxygen planes. © 2000 Academic Press

INTRODUCTION

The compound $TlSr_2CuO_5$ (hereafter, Tl-1201) is the first member ($n = 1$) of the homologous copper oxide series $TlSr_2Ca_{n-1}Cu_nO_y$; it consists of an intergrowth of double rock salt layers $[(TlO)(SrO)]_\infty$ and single $[(SrCuO_3)]_\infty$ perovskite layers (1–3). The stoichiometric compound $TlSr_2CuO_5$ is difficult to synthesize under normal conditions due to the intrinsically high copper valence (Cu^{3+}) necessary to maintain charge balance. If $TlSr_2CuO_5$ is rendered oxygen deficient, in an attempt to reduce the copper valence of the system, it transforms to an orthorhombic structure and, although metallic, shows no evidence for superconductivity down to low temperatures (4). The material has been made superconducting by the substitution of lanthanide ions for strontium (5, 6). Ohshima and coworkers (4) have reported the investigation of an oxygen-deficient $TlSr_2CuO_{5-\delta}$ phase, noting that the material was nonsuperconducting due to the large number of oxygen vacancies in the copper–oxygen planes. Furthermore, these authors stated that the location of these oxygen vacancies led to a superstructure consisting of corner-sharing CuO_6 octahedra and CuO_4 planar units.

In the course of our investigations into the series $TlSr_2Ba_2Cu_2O_7(CO_3)_{1-z}(NO_3)_z$ ($0.0 \le z \le 1.0$), we have discovered that the oxynitrate end member ($z = 1.0$) can, upon a controlled thermal decomposition, produce a Tl-1201-type compound. As formed, this Tl-1201 compound is oxygen deficient and possesses a novel superstructure in the form of a threefold repeat along the crystallographic *b*-axis. We report here the synthesis and structure determination of the title compound, the latter performed by a combination of Rietveld refinement of both neutron powder diffraction and X-ray powder diffraction data.

EXPERIMENTAL

Black, oxygen-deficient samples of $Tl_{0.75}Sr_{1.8}Ba_{0.2}CuO_y$ were prepared from high-purity $TlNO_3$, Sr_2CuO_3, hot BaO_2, and CuO consistent with the nominal starting composition of the parent oxynitrate, $TlSr_2Ba_2Cu_2O_7(NO_3)$. These powders were intimately ground, pressed into bars, and then placed into alumina tubes. The tubes were then placed in individual quartz ampoules, evacuated to 10^{-4} bar, sealed with a bench-mounted oxygen–gas torch, and introduced into a furnace operating at 850°C. The ampoules were then kept at a temperature of 850°C for 48 h, before being quenched to room temperature.

[1] To whom correspondence should be addressed.

0022-4596/00 $35.00

Initial characterization of the samples was performed using a Guinier de Wolf camera, using Cu$K\alpha_1$ radiation. Further crystallographic analyses were performed using a Philips "X-Pert" diffraction system operating in the reflection mode, with a step size of 0.02° in 2θ. These data were used to determine the unit cell parameters and perform an initial refinement of the structure using the profile refinement program DBW 3.2 (7).

Neutron powder diffraction data on these same samples were taken in backscattering mode with the high-intensity, medium-resolution POLARIS diffractometer at the ISIS Facility of the Rutherford Appleton Laboratory. The resulting powder neutron diffraction data were analyzed by the Rietveld method using the GSAS suite of programs (8). The values of the coherent scattering lengths used for the neutron diffraction data refinement were 8.79 fm for Tl, 9.3 fm for N, 7.02 fm, for Sr, 5.25 fm for Ba, 7.72 fm for Cu, and 5.81 fm for O (9). The modified pseudo-Voigt function of Larson and Von Dreele (8) was used as a profile shape function and the background was approximated using a linear equation containing Legrendre polynomials.

The results derived from the neutron diffraction study were used as a starting model for the subsequent X-ray refinement. The complementary X-ray data were recorded between 2θ values of 10° and 130° using a Siemens D5000 diffractometer fitted with a primary beam germanium monochromator and operating in transmission mode, using Cu$K\alpha_1$ radiation and a step size of 0.02° in 2θ. These data were also refined with the GSAS suite of programs (8).

Electron diffraction photographs were recorded with a JEOL 200CX electron microscope, fitted with an eucentric goniometer, and equipped with a KEVEX analyzer. The reconstruction of the reciprocal space was carried out on numerous crystallites of the sample and systematically coupled with energy-dispersive spectrometry (EDS) (10).

Magnetic measurements from room temperature of 4.2 K were taken using a Cryogenics model S100 dc SQUID magnetometer operating with a field of 10 G and an ac Lakeshore susceptometer.

RESULTS

Our Guinier de Wolf diffraction studies of the decomposition products of $TlSr_2Ba_2Cu_2O_7NO_3$ showed that the major compound produced was a Tl-1201-type phase together with barium carbonate ($BaCO_3$) and another unknown phase as impurities. A schematic representation of the idealized thermal decomposition of $TlSr_2Ba_2Cu_2O_7(CO_3)_{1-z}(NO_3)_z$ ($z = 1.0$) is given in Fig. 1. Upon comparing the nominal starting stoichiometry of $TlSr_2Ba_2Cu_2O_7(NO_3)$ with the major product phase, $Tl_{0.75}Sr_{1.8}Ba_{0.2}CuO_y$ (Fig. 1), we see that for an idealized decomposition the product phase should be of the formula $2[Tl_{0.5}(Sr_{1.0}Ba_{1.0})CuO_y]$. To determine the actual stoichiometry of our decomposition product phase, an EDS analysis was performed and averaged over several grains of the Tl-1201 material. This analysis showed a thallium:strontium:barium ratio of approximately [2.5]:[6]:[1], which corresponds to an overall chemical formula of approximately $Tl_{0.8}\ Sr_{1.8}Ba_{0.2}CuO_y$. The decomposition of $TlSr_2Ba_2Cu_2O_7(NO_3)$ into this compound therefore leaves considerable amounts of Ba and Cu unaccounted for. A comprehensive literature survey in conjunction with X-ray diffraction analysis of the possible impurity materials has only been able to highlight the presence of barium carbonate and another unidentifiable impurity phase. Clearly, this route will also generate amorphous material upon decomposition. This effect is enhanced in decomposition reactions where ionic migration is suppressed, or even prevented, by the decomposition process.

Electron diffraction (JEOL 200CX) was used to identify a starting model for the structure of the major decomposition product (10). This indicated that the unit cell of this compound is derived from the Tl-1201 parent cell, but possesses a threefold repeat along the *b*-direction, lowering the space group to *Pmmm* (Fig. 2). A set of site assignments for the atoms in the asymmetric unit was derived for this $1 \times 3 \times 1$ supercell.

Our combined Guinier de Wolf diffraction and EDS analysis studies have shown that $BaCO_3$ is present as an impurity and that the major product phase is a strontium-rich Tl-1201-type phase. This demonstrates that there is a greater occupancy by strontium than by barium of the Ba/Sr (4*v* and 2*t*) sites in our major product phase. Consequently, for the refinement from neutron diffraction data, it was decided that the occupancy of these sites would be split to contain strontium and a small percentage of barium. Thus, the initial barium occupancies were set at 0.1 and the initial strontium occupancies set to 0.9. These values were then refined while constrained to a total occupancy at each site of 1.0. For the refinement, it was also assumed that the copper sites (Cu(1) and Cu(2)) and the oxygen sites associated with the thallium, strontium, and barium atoms (O(1), O(2), O(3), and O(4)) would be fully occupied; hence, these values were fixed to 1.0. As $BaCO_3$ had been positively identified as an impurity, GSAS refinement of the model from our powder neutron data was performed using two phases, the major product phase, $Tl_{0.75}Sr_{1.8}Ba_{0.2}CuO_y$, and $BaCO_3$.

The unit cell parameters for $Tl_{0.75}Sr_{1.8}Ba_{0.2}CuO_y$ obtained from this refinement were $a = 3.7362(3)$ Å, $b = 11.5449(9)$ Å, and $c = 9.1494(8)$ Å with corresponding *R* factors of $Rwp = 4.11\%$ and $Rp = 8.3\%$. The resulting Rietveld fit is shown in Fig. 3. These results were consistent with a model of a superstructure with a threefold repeat along the *b*-axis. Schematic representations of this superstructure, calculated from the refined atom positions, are shown in Figs. 4a and 4b, which highlight the local structure distortions present in the superstructure. Specifically, the

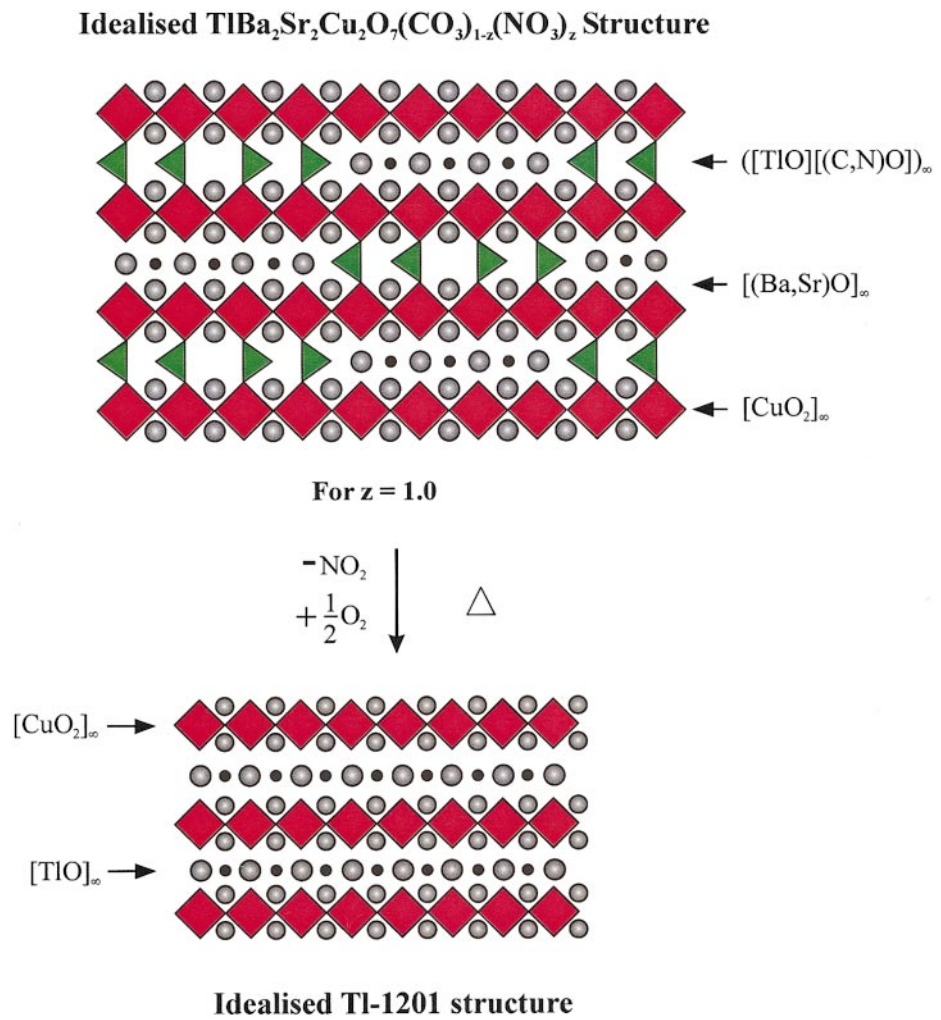

FIG. 1. A schematic representation of the decomposition of $TlSr_2Ba_2Cu_2O_7NO_3$ into $Tl_{0.75}Sr_{1.8}Ba_{0.2}CuO_y$.

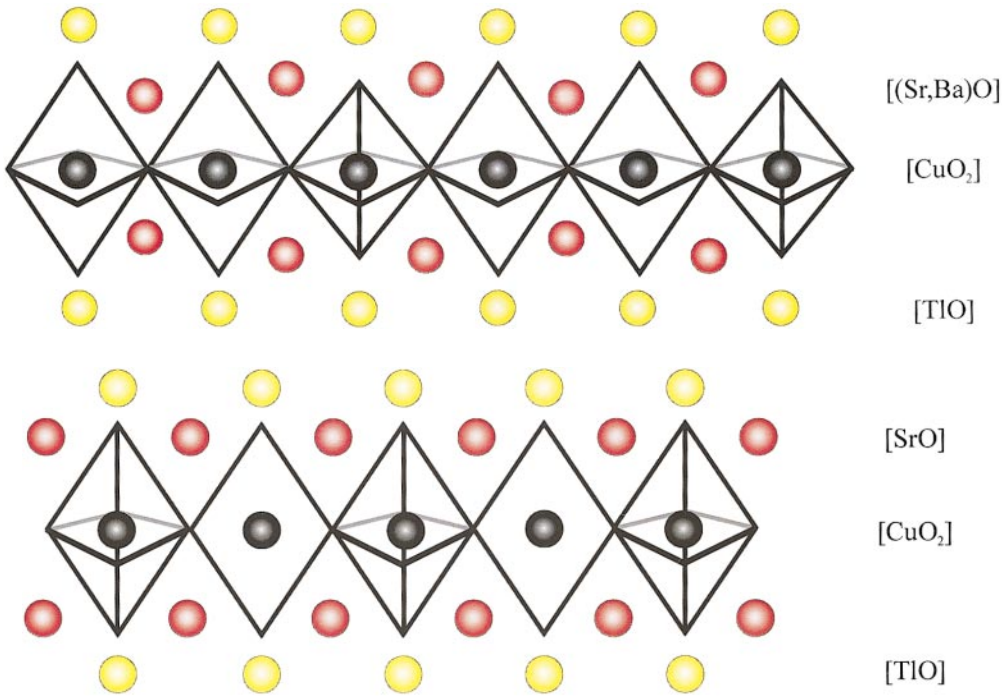

FIG. 6. (a) Schematic diagram of the threefold superstructure in Tl-1201, assuming full oxygen occupancy (this investigation). (b) Schematic diagram of the twofold superstructure in Tl-1201 taken from Ohshima *et al.* (4).

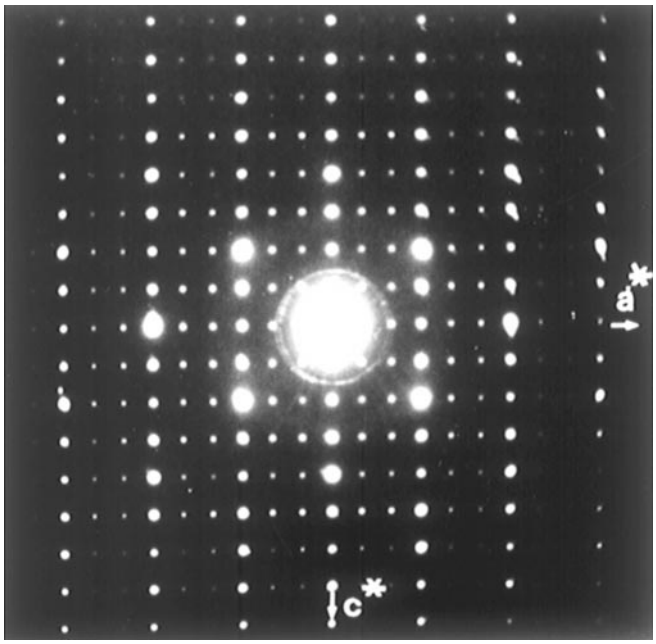

FIG. 2. A [010] electron diffraction pattern of an individual $Tl_{0.75}Sr_{1.8}Ba_{0.2}CuO_y$ crystallite.

Tl(2), Sr/Ba(1), O(3), and O(4) atoms are shown as displaced away from their "ideal" positions. It should also be noted that the refinement indicated that the O(5), O(6), and O(7) sites were not fully occupied. The structural parameters obtained from this fit have been included in Table 1, with Tables 2 and 3 showing the bond angles and bond distances, respectively.

It became apparent that the occupancy of the thallium Tl sites would refine to a value of greater than unity, which forced us to constrain the occupancy of this site to 1.0. This finding was in direct contradiction with the results from the EDS analysis, which indicated a thallium composition of approximately 0.8. This result implies the presence of a stronger neutron scatterer than Tl at this site. Given the fact that our precursor material is an oxynitrate, this could possibly be nitrogen as the nitrate ion. To test this hypothesis, further structure refinements were performed, with the occupancy of the two Tl sites split to contain thallium and a small percentage of nitrogen as a nitrate. The initial nitrate occupancy was set to 0.01 and the initial thallium occupancy set to 0.99 and these values were then refined, while constrained to a combined occupancy of 1.0. These refinements, however, failed to produce any meaningful values for the relative occupancies of thallium and nitrogen in these sites. Therefore, it seems likely that the difference (0.51 fm) between the scattering length of neutrons for nitrogen and thallium is not sufficiently large to unambiguously determine the relative occupancies of these two. The use of infrared spectroscopy to indentify the

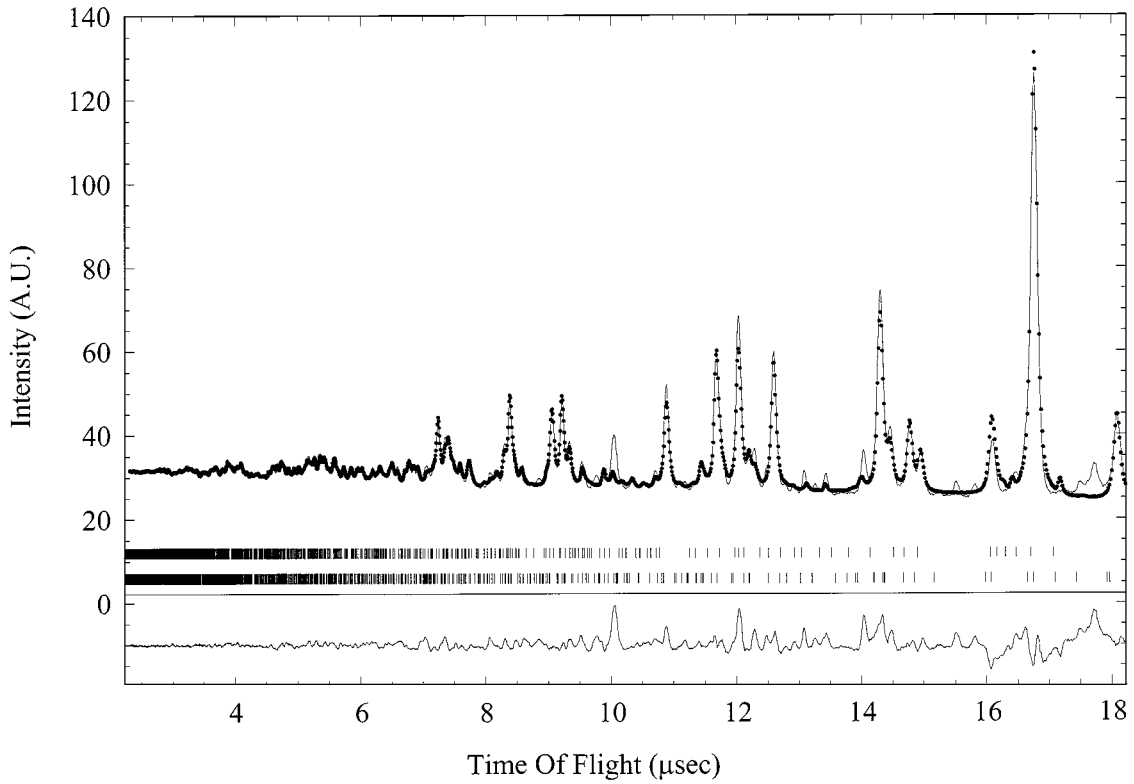

FIG. 3. Observed (full line), calculated (dotted line), and difference plots for neutron powder refinement of the superstructure of $Tl_{0.75}Sr_{1.8}Ba_{0.2}CuO_y$. The marks symbolize the Bragg angle positions for barium carbonate (top line) and $Tl_{0.75}Sr_{1.8}Ba_{0.2}CuO_y$ (bottom line).

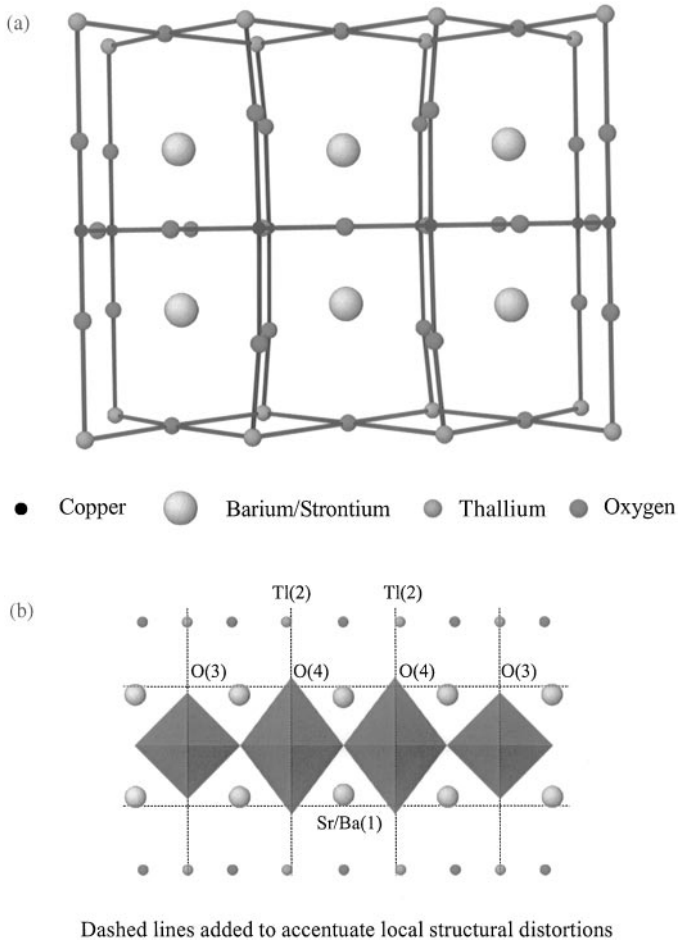

FIG. 4. (a) A schematic representation, assuming full oxygen occupancy, of the new superstructure of $Tl_{0.75}Sr_{1.8}Ba_{0.2}CuO_y$. (b) A schematic representation of the new superstructure in $Tl_{0.77}Sr_{1.8}Ba_{0.2}CuO_y$, with dashed lines highlighting the local structure disorder.

presence of the nitrate group is ruled out for these black materials.

In an attempt to identify whether there is any nitrate substitution on the thallium site and to determine the overall thallium occupancy, the same sample was then re-analyzed by X-ray powder diffraction, as there is a marked difference between the X-ray scattering powder of Tl and N ($z = 81$ and 7, respectively). The structural model derived from the neutron refinement was used as a fixed starting point for this refinement with the thallium occupancy split to contain nitrogen, as before. Only the unit cell, profile, and cation thermal parameters were subsequently refined, except that the site positions, occupancies, and thermal parameters of the Tl and N sites were also refined. For these Tl/N sites, the thermal parameters were constrained to be identical and the combined occupancies constrained to be 1.0. The unit cell parameters obtained from this refinement were $a = 3.7526(2)$ Å, $b = 11.6016(7)$ Å, and $c = 9.1898(6)$ Å, with R factors of $Rwp = 7.52\%$ and $Rp = 5.54\%$. In

TABLE 1

Structural Parameters of the Superstructure of $Tl_{0.75}Sr_{1.8}Ba_{0.2}CuO_y$ Obtained by Combined Rietveld Analysis of X-Ray and Neutron Powder Diffraction Data

Type	Mult	Frac	x	y	z	$B_{iso} \times 10^2$
Tl(1)	1*a*	0.75(3)	0.0000	0.0000	0.0000	40.9(9)
Tl(2)	2*m*	0.75(2)	0.0000	0.3206(9)	0.0000	6.6(1)
Sr(1)	4*v*	0.7773(1)[f]	0.5000	0.1664(1)[f]	0.2946(1)[f]	2.61(6)
Sr(2)	2*t*	1.0000[a]	0.5000	0.5000	0.3037(1)[f]	12.3(4)
Cu(1)	1*c*	1.0000[b]	0.0000	0.0000	0.5000	12.0(1)
Cu(2)	2*n*	1.0000[b]	0.0000	0.337(1)	0.5000	3.82(3)
O(1)	2*o*	1.0000[c]	0.5000	0.143(2)[f]	0.0000	4.47(4)[f]
O(2)	1*d*	1.0000[c]	0.5000	0.5000	0.0000	17.59(6)[f]
O(3)	2*q*	1.0000[c]	0.0000	0.0000	0.285(1)[f]	0.88(2)[f]
O(4)	4*u*	1.0000[c]	0.0000	0.334(2)[f]	0.224(1)[f]	28.9(2)[f]
O(5)	1*d*	0.632[f]	0.5000	0.0000	0.5000	5.0[e]
O(6)	2*p*	0.580[f]	0.5000	0.333(3)[f]	0.5000	0.245(4)[f]
O(7)	2*n*	0.947[f]	0.0000	0.169(1)[f]	0.5000	1.25(2)[f]
O(8)	1*g*	1.0000[a]	0.0000	0.5000	0.5000	5.0[e]
Ba(1)	4*v*	0.2227(1)	0.5000	0.1664(1)[f]	0.2946(1)[f]	2.61(6)
Ba(2)	2*t*	0.0000[d]	0.5000	0.5000	0.3037(1)[f]	12.3(4)
N(1)	1*a*	0.25(3)	0.0000	0.0000	0.0000	40.9(9)
N(2)	2*m*	0.25(2)	0.0000	0.3206(9)	0.0000	6.6(1)

Lattice constants

$a = 3.7362(3)$ Å $b = 11.5449(9)$ Å $c = 9.1494(8)$ Å (neutron)
$a = 3.7526(2)$ Å $b = 11.6016(7)$ Å $c = 9.1898(6)$ Å (combined X-ray and neutron)
$\alpha = 90°$ $\beta = 90°$ $\gamma = 90°$

R-Values

$Rwp = 4.11\%$ $Rp = 8.3$ (neutron)
$Rwp = 7.52\%$ $Rp = 5.54\%$ (combined X-ray and neutron)

$$Rwp = \left[\frac{\sum |(w_i(Y_i(\text{obs}) - (1/c)\,Y_i(\text{calc}))^2|}{w_i \sum Y_i(\text{obs})^2}\right]$$

$$Rp = \left[\frac{\sum |(Y_i(\text{obs}) - (1/c)\,Y_i(\text{calc})|}{\sum Y_i(\text{obs})}\right]$$

Where Y_i(obs) and Y_i(calc) are the observed and calculated profile intensities, w_i is the least squares weight, and c is the scale factor.

[a] Previously refined to 1.0.
[b] Copper occupancy held at 1.0.
[c] Oxygen associated with Tl/Ba/Sr. Held at 1.0.
[d] Previously refined to 0.0.
[e] Not refined.
[f] From refinement of neutron data.

Fig. 5 we show the X-ray diffraction Rietveld refinement pattern for $Tl_{0.75}Sr_{1.8}Ba_{0.2}CuO_y$ and in Table 1 we list the combined neutron and X-ray refined structural parameters. Upon repeating this refinement with an absence of nitrogen (and fixed thallium thermal parameters), a slightly increased overall thallium content (0.78) was obtained, with the Rp and Rwp values remaining the same. These values for thallium occupancy agree well with the results of our EDS analysis (0.8). These refinements also provide strong support for our hypothesis that a strong neutron scatterer but corre-

TABLE 2

Bond Angles for the Superstructure of $Tl_{0.75}Sr_{1.8}Ba_{0.2}CuO_y$ Obtained by the Combined Rietveld Analysis of X-Ray and Neutron Powder Diffraction Data

Bond	Angle
Tl(1)–O(1)–Tl(1)	97.1(8)°
Tl(1)–O(1)–Tl(2)	97.0(2)°
Tl(1)–O(3)–Cu(1)	180°
Tl(2)–O(2)–Tl(2)	97.3(7)°
Tl(2)–O(4)–Cu(2)	175.3(3)°
Ba/Sr(1)–O(4)–Ba/Sr(2)	151.3(5)°
Ba/Sr(1)–O(3)–Ba/Sr(1)	176.4(6)°
Cu(1)–O(5)–Cu(1)	180°
Cu(1)–O(7)–Cu(2)	180°
Cu(2)–O(8)–Cu(2)	180°
Cu(2)–O(6)–Cu(2)	176.9(3)°

TABLE 3

Bond Distances for the Superstructure of $Tl_{0.75}Sr_{1.8}Ba_{0.2}CuO_y$ Obtained by the Combined Rietveld Analysis of X-Ray and Neutron Powder Diffraction Data

Bond	Distance (Å)
Tl(1)–O(1)	2.5037(2)
Tl(1)–O(3)	2.6182(3)
Tl(2)–O(1)	2.788(8)
Tl(2)–O(2)	2.799(8)
Tl(2)–O(4)	2.0635(8)
Ba/Sr(1)–O(1)	2.7200(3)
Ba/Sr(1)–O(3)	2.6926(2)
Ba/Sr(1)–O(4)	2.7779(2)
Ba/Sr(1)–O(5)	2.6991(2)
Ba/Sr(1)–O(6)	2.7007(2)
Ba/Sr(1)–O(7)	2.6607(2)
Ba/Sr(2)–O(2)	2.7900(3)
Ba/Sr(2)–O(4)	2.7825(2)
Ba/Sr(2)–O(6)	2.6464(2)
Ba/Sr(2)–O(8)	2.6019(2)
Cu(1)–O(3)	1.9752(2)
Cu(1)–O(5)	1.8757(2)
Cu(1)–O(7)	1.9600(2)
Cu(2)–O(4)	2.5358(2)
Cu(2)–O(6)	1.8762(2)
Cu(2)–O(7)	1.9484(2)
Cu(2)–O(8)	1.8904(2)

spondingly weak X-ray scatterer, i.e., nitrogen, occupies the Tl sites.

DISCUSSION

The proposed superstructure takes the form of a threefold repeat along the *b*-axis. From the combined neutron and X-ray refinement (Table 1) it can be seen that this superstructure is produced primarily from local distortions of the Tl(2) and Ba/Sr(2) atoms away from their ideal positions. Schematic diagrams illustrating the superstructure and these distortions are shown in Fig. 4a and 4b, respectively. The [010] electron diffraction pattern of this phase shown in Fig. 2 provides clear evidence that a threefold repeat is indeed present. The refinement also indicates that both the O(5) and O(6) have extremely low occupancies (of

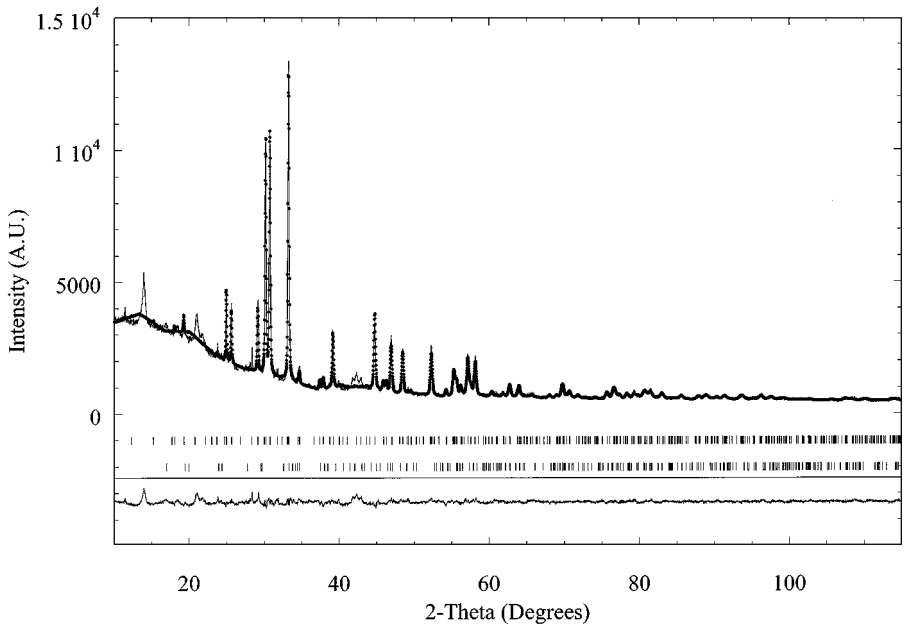

FIG. 5. Observed (full line), calculated (dotted line), and difference plots for X-ray powder refinement of the superstructure of $Tl_{0.75}Sr_{1.8}Ba_{0.2}CuO_y$. The marks symbolize the Bragg angle positions for $Tl_{0.77}Sr_{1.8}Ba_{0.2}CuO_y$ (top line) and barium carbonate (bottom line).

the order of 0.6). This produces severe disruption of the Cu–O plane and presumably prevents the appearance of any superconducting properties.

The proposed superstructure derived from this investigation (Fig. 6a) is compared with that of Ohshima *et al.* (4), who reported a twofold repeat along the *b*-axis, consisting of a CuO_4–CuO_6 repeat (Fig. 6b) with unit cell parameters of $a = 3.6607(5)$ Å, $b = 7.5709(11)$ Å, and $c = 8.9672(13)$ Å. The change from twofold to threefold repeating units can clearly be seen in the *b* lattice dimension, which is 30% larger for our material than for that of Ohshima and co-workers. The increase in the *a* and *c* parameters for our material over those observed by Ohshima are considered to be due to the partial substitution of the strontium cation with the larger barium cation ($Sr^{2+} = 1.12$ Å, $Ba^{2+} = 1.34$ Å).

We found no evidence for superconductivity in this material down to 4.2 K. This was almost certainly due to the fact that the majority of the oxygen vacancies occur in the copper–oxygen plane (O(5), O(6), and O(7)), thus disrupting the extended copper–oxygen interaction necessary for electronic conduction.

CONCLUDING REMARKS

We have illustrated that the controlled decomposition of the oxynitrate material, $TlSr_2Ba_2Cu_3O_7NO_3$, leads to the production of a Tl-1201 material, which has been identified by neutron powder diffraction as being of the general formula $Tl_{0.75}Sr_{1.8}Ba_{0.2}CuO_y$. Furthermore, this Tl-1201 phase was shown to possess a complicated superstructure consisting of a threefold repeat along the *b*-axis, brought about by the local distortions in the structure. A combination X-ray and neutron refinement seems to indicate that there may be partial occupation of the thallium layer by nitrogen, in the form of nitrate groups.

The material is nonsuperconducting presumably due to the large number of vacancies in the copper–oxygen planes, which disrupts the Cu–O–Cu interaction and inhibits the super exchange pathway necessary for superconductivity.

ACKNOWLEDGMENTS

The authors are grateful to A. Maignan of Laboratoire CRISMAT, Caen and M. Slaski of the Department of Physics and Space Research, Birmingham, for running low-temperature magnetic measurements. This work was supported by grants from the European Union (Network ERB CHRX-CT940461) and the E.P.S.R.C.

REFERENCES

1. A. K. Ganguli and M. A. Subramanian, *J. Solid State Chem.* **93,** 250 (1991).
2. T. Kaneko, T. Wada, A. Ichinose, H. Yamauchi, and S. Tanaka, *Physica C* **177,** 153 (1991).
3. E. Ohshima, M. Kikuchi, M. Nagoshi, R. Suzuki, S. Nakajima, K. Nagase, and Y. Syono, *Physica C* **214,** 182 (1993).
4. E. Ohshima, M. Kikuchi, F. Izumi, K. Hiraga, T. Oku, S. Nakajima, N. Ohnishi, Y. Morii, S. Funahashi, and Y. Syono, *Physica C* **221,** 261 (1994).
5. M. H. Whangbo and M. A. Subramanian, *J. Solid State Chem.* **91,** 403 (1991).
6. M. Huve, C. Michel, C. Martin, M. Hervieu, A. Maignan, J. Provost, and B. Raveau, *Physica C* **179,** 214 (1991).
7. D. B. Wiles and R. A. Young, *J. Appl. Crystallogr.* **14,** 149 (1981).
8. A. C. Larson and R. B. Von Dreele, "General Structure Analysis System." University of California, 1985–1990.
9. V. F. Sears, *Neutron News* **3,** 26 (1992).
10. M. O. Jones, M. Hervieu, C. Michel, P. P. Edwards, and B. Raveau, in preparation.